Estimation of trial parameters for Pulse Phase Thermography with low power heat sources

L Vitali, D Fustinoni, **P Gramazio and A Niro**

Energy Department, Politecnico di Milano,
Campus Bovisa, Via Lambruschini 4, 20156 Milano – ITALIA

E-mail: luigi.vitali@mail.polimi.it

Abstract. Non-destructive Testing (NDT) by Infrared Thermography is a widely adopted technique to reveal the presence of defects, i.e. discontinuity zones of thermal proprieties, inside materials. Pulsed Phase Thermography (PPT) is one of the most interesting techniques among IR-NDT: the specimen is heated by a thermal pulse and the sequence of thermograms of the surface cooling is transformed with the Discrete Fourier Transform (DFT). The resulting phase images (phasegrams) show little sensitivity to irregular heating and surface proprieties, and allow better defect identification by increasing the contrast. It is also possible to estimate the depth of the defect by correlating a characteristic frequency to the thermal diffusion length of the defect. The outcome of this analysis depends on the fine tuning of the technique and the appropriate choice of the parameters of the thermal pulse, namely length and power, as well as of the acquisition, i.e. frequency and observation time. While there are in literature a few guidelines for the choice of these parameters, a good knowledge of the technique and a certain degree of guessing is still required, especially when low heating power, longer pulses and small and deep defects are involved. This paper reports a method to estimate these parameters, partly based on theoretic considerations and partly on numerical simulations performed by means of a FEM commercial code on a 2D axial-symmetric model. Experimental results are also here presented, focusing on the difference between a thick plate and a thin one.

1. Introduction

Pulsed Phase Thermography (PPT) is a widely studied and used technique regarding the non destructive assessment of discontinuities within a huge range of materials and thicknesses, from concrete walls to metal or composite plates used in various engineering applications. Its main advantages are a low sensitivity to uneven heating and specimen emissivity, and a better identification of deeper defects compared to the time based Pulse Thermography techniques.

A lot of studies focusing on specific applications are available in the open literature, but only a few are about the correct choice of the trial parameters ([1], [2]). Indeed, these parameters are crucial for a successful test execution, especially when the PPT is carried out with halogen lamps whose pulse can not be shorter than a few seconds in order to efficiently heat the specimen. The present work reports about a way to readily estimate these parameters, i.e., pulse length and power, observation time and frequency, via a combination of theoretical and numerical approaches, experimentally validated on polymethylmethacrylate specimens.

2. Theory

The 1D model of thermal pseudo-waves propagation (solution of a diffusion equation) is still used today as a basis to understand the behavior of the phenomenon under study [3], combined with knowledge about how thermal pseudo-waves reflect and refract on obstacles according to the Snell law [4].

Let us consider a very thick slab, and let us impose an harmonic heat flux boundary condition on one of its surfaces:

$$q(0,t) = T_0 \cos(2\pi f t - \varphi)$$

If we further assume that inside the slab there is a defect like a delamination at a depth L, the resulting surface temperature estimated for a 1D model is

$$T(0,t) = T_0 \cos(2\pi f t - \varphi - \pi/4) + \hat{r} T_0 e^{-2L/\mu} \cos\left(2\pi f t - \frac{2L}{\mu} - \varphi\right)$$

The factor μ is the *thermal diffusion length*, defined as

$$\mu = \sqrt{\frac{\alpha}{\pi f}}$$

that expresses how deep a thermal wave can travel inside a medium (for $z = \mu$ the amplitude is reduced by a factor *1/e*), and $\hat{r}$ is the reflection coefficient

$$\hat{r} = \frac{e_1 - e_2}{e_1 + e_2}$$

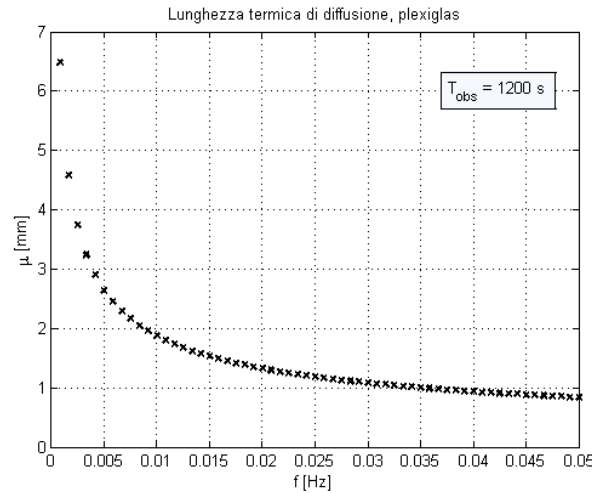that depends on the effusivity of both the specimen and the defect.

Figure 1. Thermal diffusion length, Plexiglas, fixed observation time

Although the 1D model is useful to understand the basic behavior of the phenomenon, it is quite inaccurate for prediction purposes, because the 2D and 3D effects, depending on the defect shape, cannot be ignored. In considering this, several analytical models have been proposed, especially in order to take into account the lateral size of the defect [5], and the effect of surface convection [3].

3. Experiments

3.1. Experimental setup

The experimental setup is made by two reflectors, each one equipped with a 500W halogen lamp and a guillotine shutter in order to ensure a thermal square pulse to a good extent. The IR camera is the Raytheon Radiance HS (InSb, Focal Plane Array, detectable wavelength region 3-5 μm). Experiments are carried out using specimens, that are PMMA flat plates with two thickness, namely, 4 and 20 mm, respectively. On one side, flat-bottomed holes are drilled to simulate the defects, while the other is black painted to enhance its emissivity.
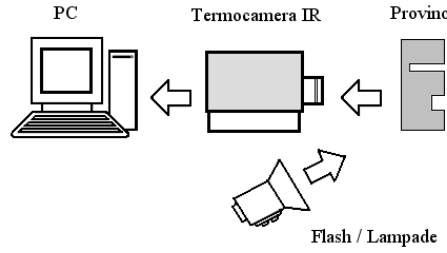

Figure 2. Experimental scheme

Table 1. Thermal proprieties

PMMA		
Density	ρ [kg/m^3]	1190
Specific heat capacity	c [J/(kg K)]	1470
Thermal conductivity	k [W/(m K)]	0.19
Thermal diffusivity	α [mm^2/s]	0.109

3.2. Inversion method

The inversion method used in this work was proposed by Gutierrez-Fajardo in [6]. It is observed that, for each defect depth, there is an optimal visibility frequency (f_{opt}) at which the defect appears the least distorted or affected by noise. In order to find this frequency, a correlation function R between consecutive phasegrams $\Phi_i(f_i)$ is calculated, according to the following equations.

$$r(A, B) = \frac{\sum_{i=1}^{Row} \sum_{j=1}^{Col} (A_{ij} - \bar{A})(B_{ij} - \bar{B})}{\sqrt{\left(\sum_{i=1}^{Row} \sum_{j=1}^{Col} (A_{ij} - \bar{A})^2\right)\left(\sum_{i=1}^{Row} \sum_{j=1}^{Col} (B_{ij} - \bar{B})^2\right)}} \tag{1}$$

$$R = \left[r(\Phi_1, \Phi_2),\ \ r(\Phi_2, \Phi_3), \dots r(\Phi_i, \Phi_{i+1}), \dots r\left(\Phi_{\frac{N}{2}-1}, \Phi_{\frac{N}{2}}\right) \right] \tag{2}$$

The frequency at which R(f) is maximum (the lowest of the two for first five pairs of phasegrams, the average for the rest) goes into the following equation (3) that gives the defect depth.

$$z_{exp} = C1 \sqrt{\frac{\alpha}{\pi f_{Rmax}}} \tag{3}$$

C1 is a correlation constant obtained by set of trials on known depth defects, and that could depend on the specimen material [2].

This criterion showed good results specially for the deepest defects that are associated to the lowest frequencies, because of a lower phase noise; and further, it has the advantage that the user has not to point at a sound zone.

3.3. Experimental procedure

3.3.1. Pulse. The power spectrum of an ideal $\delta(t)$ pulse is a constant, i.e, every frequency is excited with the same intensity. However, actual thermal pulses have a finite duration; while a 5 ms flash can be considered quite an ideal pulse for our purposes, pulse time τ is in the order of seconds when lamps are used, and it must be carefully selected in order to properly stimulate the highest frequencies associated with the most superficial flaws. Indeed, the longer the pulse times, the larger the power on low frequencies, and, as a consequence, they are well suited for deeper investigations.

$$q(t) = \begin{cases} 0 & t \leq 0 \\ q_0 & 0 < t \leq \tau \\ 0 & t > \tau \end{cases}$$
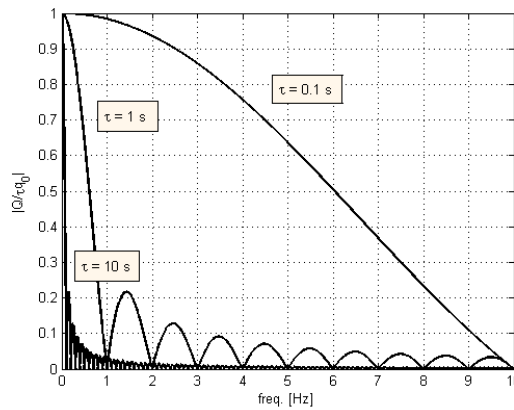

Figure 3. Energy distribution for various pulses, normalized

3.3.2. Postprocessing. Data acquired from the IR camera is automatically processed with a dedicated software developed by ThermALab following this procedure.
- Calibration from grayscale to temperature values; the calibration is carried out with a blackbody and it is normally non-linear.
- FFT for each pixel, obtaining N/2 phasegrams.
- Median and Gaussian filters on each phasegram, in order to reduce crazy pixels and high frequency noise respectively.
- Morphological reconstruction [6]. This technique is based on the *image segmentation*, i.e., the division of an image into different regions (minima and maxima of phase) in order to use geodesic dilatation and erosion algorithms to extract both shape and extension of the defect from the phasegram image
- Correlation between phasegrams, according to equation (1)

4. Numerical simulations

4.1. Numerical model

A numerical FEM model has been developed to quickly evaluate the trial parameters, as well as the constant *C1* in equation (3), while taking into account different materials or defect types, i.e., different reflection coefficients.

The model is characterized by a 2D axisymmetric geometry, and it is equivalent to a round plate with the defect located at its center. The points whose temperatures are extracted are the one on the center of the defect and that located 4.5 mm from the symmetry axis, respectively.

4.2. Validation

The model should reproduce the behavior of the sound zone. The analysis on the 20 mm thick specimen shows a good agreement between experimental and predicted data, even for the simplest possible model, whose boundary condition are adiabatic on every sides (figure 2).
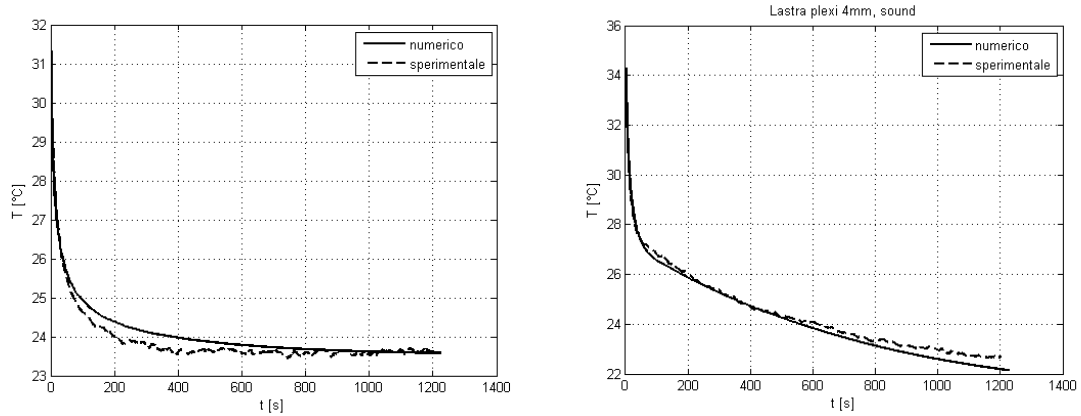

Figure 2. numerical vs. experimental data on sound specimens

The 4 mm thick specimen requires instead that heat losses have to be taken into account. To this end, convective heat transfer boundary condition with $h=5$ W/(m^{2}K) was introduced. By means of the model, the FFT of the temperature can be calculated, and the defect depth can be evaluated by the frequency at which the phase difference shows a maximum in equation (2).

A validation was carried out by comparisons with results from literature [2] of the behavior of the phase difference $\Delta\varphi$ between the defect centre and the sound zone, varying the depth and the size of the defect. This model clearly shows the expected results, namely the defect size only affects the magnitude of $\Delta\varphi$, whereas the correspondent frequency doesn't change. On the other end, an increase of depth causes a decrease of the frequency at which $\Delta\varphi$ peaks.
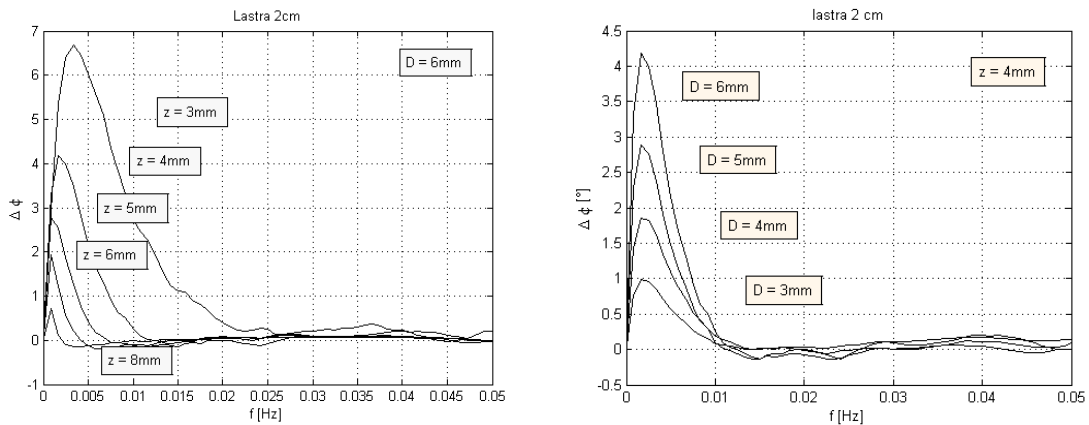

Figure 4. Phase differences varying defect dimensions

4.3. Automatic regression

The simple FEM model here developed shows good results and has a fast execution time. So, a routine has been written to evaluate, given a set of defects, namely diameters and depths, an estimate of the main parameters of interest. In particular, the correlation coefficient C1, whose evaluation requires normally an experimental campaign on a set of known flaws, the influence of the trial parameters on depth estimation errors and, given the IR camera sensitivity, an indication about which defects are detectable, by showing the times at when a temperature difference between the flow and the sound zone is measurable.

Table 2. Automatic regression output

E	Tau	Mat	thickness	T_oss [s]	Coeff.	σ	CONV	IR Cam sens.	
1350	20	plex/aria	4mm	1200	1,077	0,32715	SI	0,15	

Z	D	μ_{num}	z_{num}	$\Delta\phi_{max}$	n_freq	f_Δf max	t_{start}	t_{end}	errore
2	4	1,53	1,65	4,88	19	0,015	1	174	17,73
2	8	2,16	2,33	13,42	10	0,0075	1	361	-16,35
2	12	2,29	2,47	18,94	9	0,006667	1	504	-23,41
5	4	4,58	4,94	0,99	3	0,001667	0	0	1,27
5	8	4,58	4,94	3,96	3	0,001667	75	315	1,27
5	12	4,58	4,94	7,54	3	0,001667	55	577	1,27
7	4	6,48	6,98	0,46	2	0,000833	0	0	0,27
7	8	6,48	6,98	1,99	2	0,000833	0	0	0,27
7	12	6,48	6,98	4,30	2	0,000833	235	389	0,27

5. Estimation of parameters

5.1. Pulse

5.1.1. Pulse. The frequency of the first zero of the square pulse Fourier transform is $f_0 = 1/\tau_I$. Our criterion is that the desired frequency range should fall below the 50% of the main lobe in order to receive enough energy. Therefore, the automatic regression is run to find the maximum estimated frequencies associated with low-depth defects.

$$\tau_I = \frac{1}{2 \max(f_{\Delta\varphi max})}$$

5.1.2. Power. In [5] it is shown that the power of the thermal stimulus is proportional to the temperature contrast between the sound and the defect zones. As already observed, the program shows which defects are detectable for a certain power, and it can be used to evaluate whether a more powerful apparatus is required.

5.2. Acquisition

5.2.1. Sampling frequency. The sampling frequency must be chosen according to the Nyquist criterion as well as to the possible presence of aliasing [6]. To our purposes, for low thermal conductivity materials, frequencies involved are low and a sampling rate of 1Hz is typically adopted.

5.2.2. Observation time. The observation time must assure a good resolution at low frequencies for thick materials and it must be long enough to observe the complete cooling transient during which a temperature difference between the defect and the sound zones is measurable.

By means of the regression program, the used criterion is

$$t_{oss} = 1.25 \ t_{end}$$

where t_{end} is the time when a temperature difference between defected and sound zones is no longer detectable for the type of flaws that has to be investigated.

6. Experimental results

The adopted technique shows good results when applied on the 2 cm thick specimen. The depth measurement error, defined as

$$err = \frac{z_{exp} - z}{z}$$

is extremely low ($< 0.3\%$) for the considered defects. The rule of thumb, that the defect diameter should be equal to or greater than its depth for appropriate detection and identification, is partly confirmed, i.e., the defect D4z7 is not detectable.

Table 3. Experimental results, 2 cm plate

D [mm]	z [mm]	z_{exp} [mm]	err %
8	2,5	3,17	0,27
8	4	5,22	0,31
8	6	6,18	0,03
8	8	7,98	-0,00
6	6	6,18	0,03
4	3	3,83	0,28
4	5	5,22	0,04
4	7	x	x
10	10	9,77	-0,02

The 4 mm thick plate shows a few peculiar issues. All defects besides D2z3 are visible, but the most superficial defects are not clearly identifiable, due to the high phase noise at higher frequencies.

The technique shows instead very good results for 2 mm and 3 mm deep defects.

Table 4. Experimental results, 4mm plate

D[mm]	z[mm]	z_{exp}[mm]	err	Note
6	2	2.04	20	good characterization
6	3	3.03	10	visible only in phase images
4	1	n.a.	n.a.	visible but not identifiable
4	2	2.08	40	
4	3	3.03	10	
2	1	n.a.	n.a.	visible but not identifiable
2	2	n.a.	n.a.	visible but not identifiable
2	3	n.a.	n.a.	not visible

7. Conclusions

A Numerical and experimental analysis have been carried out to better understand the pulse phase thermography mechanism. In particular, our analysis have been focused on the limitations of the use of conventional lamps instead of flashes.

A numerical model has been developed to predict the behavior of the defect set as well as to estimate the trial parameters and the correlation constant *C1* between the defect depth and the thermal diffusion length.

The technique adopted at the ThermALab at Politecnico di Milano has been presented, and in particular the phasegram correlation criterion to identify the frequency associated with the defect depth has been discussed.

Finally, it has been shown that the deepest defects, i.e., up to 10 mm, in low-conductivity materials are precisely identifiable, while defects just below the surface, i.e., 1 mm deep are visible but not yet identifiable at this time.

References

[1] Marinetti S, Plotnikov Y A, Winfree W P, Braggiotti A 1999 *proc. of SPIE* **3586** 230–38
[2] Ibarra Castanedo C 2005 *Quantitative subsurface defect evaluation by pulsed phase thermography: depth retrieval with phase*, phd. Thesis, Université Laval
[3] Ishikawa M, Hatta H, Habuka Y, Fukui R, Utsunomiya S 2013 *IR Phys. & Tech.* **57** 42-49
[4] Bertolotti M, Liakhou G L, Li Voti R, Paoloni S, Sibilla C 1999 *J Appl Phys*, **85**(7)
[5] Almond D P and Pickering S G 2012 *J. Appl. Phys.* **111**, 093510
[6] Gutiérrez Fajardo A 2005 *An Analytical and experimental study on defect recognition methodologies with Pulse Phase Thermography*, MS Thesis, Politecnico di Milano
[7] Lau S K, Almond D P and Milne J M 1991 NDT&E Int. **24** 040195-08
[8] Shepard S M, Lhota J R and Ahmed T 2009 *Proc. of SPIE* **7299**0T 1-7